

CONTINUOUS OPTIMIZATION FOR FIELDS OF EXPERTS DENOISING WORKS

PETTER STRANDMARK AND SAMEER AGARWAL

ABSTRACT. Several recent papers use image denoising with a Fields of Experts prior to benchmark discrete optimization methods [5, 6, 7, 8, 10, 11, 15]. We show that a non-linear least squares solver significantly outperforms all known discrete methods on this problem.

1. INTRODUCTION

For many optimization problems, a local model built using derivatives simply does not give any useful information about the global structure, making it hard for continuous methods to find good solutions. For some of these problems, the discrete optimization methods commonly used in computer vision and image analysis are able to avoid undesired local minima; see [2, 4].

Fields of Experts (FoE) is a sophisticated prior on the statistics of natural images [16]. It has a larger clique structure that is capable of capturing higher order interactions around each image pixel than models based on pairwise interactions. One area where the FoE priors have been used to great success is image denoising. For example, the recent state-of-the-art results in image denoising [9] use FoE as one part in a more complicated machine learning system.

There seems to be a general sense that MAP inference in problems arising from the use of FoE models is hard and that continuous optimization methods may not be suitable for it. Thus an increasingly sophisticated (and expensive) array of discrete optimization methods have been developed to solve them [5, 6, 7, 8, 10, 11, 15]. In this short paper we argue that a simple continuous optimization method can be used to solve the FoE denoising problem cheaply and effectively. We provide an open-source implementation of this method.

2. DENOISING USING FIELDS OF EXPERTS

Given a noisy image \mathbf{u} , the negative log-likelihood for an image \mathbf{x} using the FoE prior is

$$(1) \quad f(\mathbf{x}) = \sum_{i=1}^n \frac{(x_i - u_i)^2}{2\sigma^2} + \sum_{P \in \mathcal{P}} \sum_{k=1}^K \alpha_k \log \left(1 + \frac{1}{2} \left(\mathbf{b}_k^T \mathbf{x}_P \right)^2 \right),$$

where P is an image patch in the set of all $m \times m$ patches \mathcal{P} of \mathbf{x} and σ is the standard deviation of the Gaussian noise in \mathbf{u} . The coefficients α_k and the filters \mathbf{b}_k for $k = 1, \dots, K$ are estimated from a database of natural images [16]. This, the problem of denoising \mathbf{u} can be formulated as the finding image \mathbf{x} that minimizes (1).

Method		test001		test002		test003		test004	
		obj.	time	obj.	time	obj.	time	obj.	time
As reported in [7]	[6, 8]	37769	1326 s.	25030	1330 s.	29805	1305 s.	27356	1290 s.
	[7]	38132	71 s.	24831	81 s.	29683	67 s.	27354	79 s.
On our computer	[6, 8]	37691	625 s.	24997	631 s.	29762	623 s.	27330	604 s.
	[7]	37686	16 s.	25129	24 s.	29734	22 s.	27219	18 s.
	Levenberg-Marquardt	37374	2 s.	24556	2 s.	29434	2 s.	27088	2 s.

TABLE 1. Denoising the four 160×240 test images used in [6, 7, 8] (shown in Fig. 1) with 2×2 filters, $K = 3$ and $\sigma = 20$. The table reports final objective function values and running times.

3. FUSION MOVES

Fusion move is a common discrete optimization method used in image analysis [12]. Let $\mathbf{p}, \mathbf{q} \in \mathbf{R}^n$ be two candidate solutions to a minimization problem $\min_{\mathbf{x} \in \mathbf{R}^n} f(\mathbf{x})$. A new solution can be formed by picking (“fusing”) components from \mathbf{p} and \mathbf{q} independently according to an indicator vector \mathbf{z} :

$$(2) \quad \min_{\mathbf{z} \in \{0,1\}^n} f\left((1 - \mathbf{z}) \cdot \mathbf{p} + \mathbf{z} \cdot \mathbf{q}\right).$$

Computing the optimal \mathbf{z} is a discrete optimization problem which can be solved using roof duality [10, 12]. This framework includes α -expansion [2] as a special case.

All of the fastest reported methods for minimizing (1) are based on fusion moves [5, 6, 7, 8]. Generating good candidates is crucial and can be done in many ways. Two types of candidates have been used for FoE denoising: (i) blurring and randomly perturbing a current solution [6, 8] and (ii) generating a candidate from the gradient of the objective function [7].

4. NON-LINEAR LEAST SQUARES

A robustified nonlinear least squares problem is the minimization of a function of the form [1]:

$$(3) \quad \sum_{i=1}^N \rho_i \left(\|f_i(\mathbf{x}_{P_i})\|^2 \right).$$

Here, ρ_i is a *loss function*. If it is the identity function, the problem is an ordinary non-linear least squares problem. Otherwise, under some mild conditions on ρ_i , (3) can still be solved using a non-linear least squares algorithm after appropriate modifications to the residual vector and the Jacobian matrix [17].

Observe that the first sum in (1) can be written in the form of (3) by setting

$$(4) \quad f_i(x) = \frac{x - u_i}{\sqrt{2}\sigma} \quad \text{and} \quad \rho_i(s) = s,$$

and the second sum by setting

$$(5) \quad f_k(\mathbf{x}_P) = \mathbf{b}_k^T \mathbf{x}_P \quad \text{and} \quad \rho_k(s) = \alpha_k \log \left(1 + \frac{s}{2} \right).$$

Thus, (1) is a robustified non-linear least squares problem.



FIGURE 1. The four denoised test images using a 2×2 FoE model. Table 1 shows the quantitative results.

Method	test001		test002		test003		test004	
	obj.	time	obj.	time	obj.	time	obj.	time
Levenberg-Marquardt, 3×3 , $K = 8$	55186	25 s.	39750	24 s.	44798	25 s.	42367	20 s.
Levenberg-Marquardt, 5×5 , $K = 24$	61304	132 s.	42518	139 s.	47093	149 s.	44820	113 s.

TABLE 2. Denoising with higher-order FoE models using the noisy images in Fig. 1. The objective function values are from different optimization problems and are therefore not comparable.

5. EXPERIMENTS

5.1. Setup. We used CERES SOLVER [1] with the Levenberg-Marquardt algorithm [14] in combination with the CHOLMOD sparse Cholesky factorization library [3] to minimize the robustified non-linear least squares formulation of (1). We compare this to two state-of-the-art discrete optimization methods [7, 8]. The code for [8] is publicly available and we implemented [7] ourselves.

In our experiments, we used the noisy image as the initial point for the solver. Since the discrete methods use integer images, we rounded the continuous solution for the 2×2 filters to the nearest integer in $\{0, \dots, 255\}$ to get a fair comparison. This increased the final objective function value a little bit ($< 0.2\%$). All of the experiments were performed on a 3.47 GHz Intel Xeon and did not use any multi-threaded capabilities.

5.2. Results. We begin by denoising four test images using the 2×2 FoE model that has been commonly used for evaluating discrete methods. Table 1 shows the results, both as reported in [7] and of our own experiments and Fig. 1 illustrates

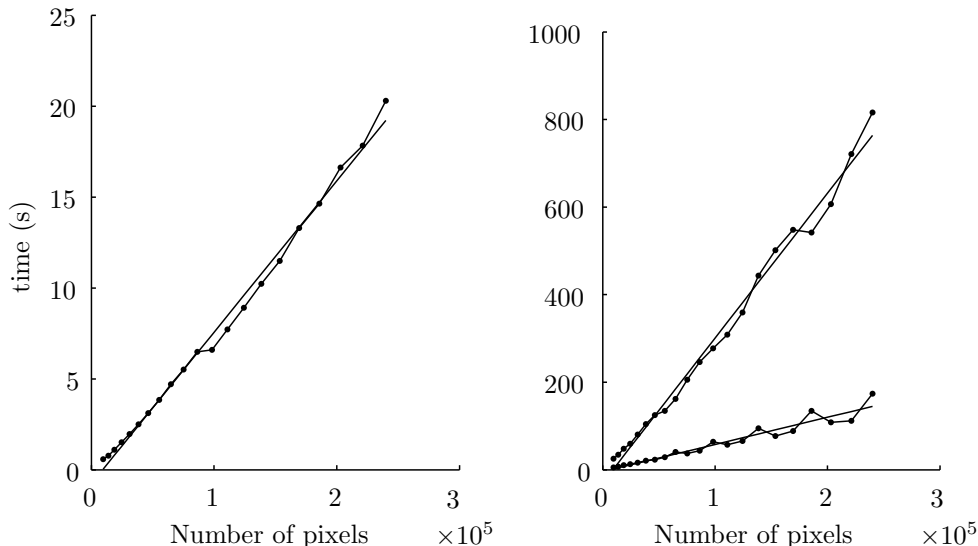


FIGURE 2. The time required to denoise an image is approximately linear in the number of pixels. The figure shows graphs for 2×2 (left), 3×3 and 5×5 (right) filters.

the minima we found. The non-linear least squares solver finds a lower objective function value at a fraction of the runtime of the discrete methods.

Apart from the four test images used for benchmarking in previous publications, we added noise to the 100 test images in the Berkeley Segmentation Database [13]. The non-linear least squares solver always found a better objective value than the method in [7] (1% on average) and was much faster (11 and 100 seconds, respectively, on average).

Because of limitations of the methods used for pseudo-boolean optimization, discrete methods for FoE inference have focused on the 2×2 case. The methods in [5], [8] and [10] are not capable of handling the degree-9 polynomials that would be required for 3×3 inference. In contrast, nothing is preventing a nonlinear least squares solver from using 3×3 or 5×5 filters. Table 2 contains our running times and final objective function values for the four test images.

Finally, we performed an experiment where we resized an image to different sizes, added noise, and denoised it using the nonlinear solver. Figure 2 shows that the running time is approximately linear in the number of pixels.

6. DISCUSSION

Non-linear least squares performs very well when applied to MAP Fields of Experts denoising. It is several times faster than the fastest method based on discrete optimization and it is immediately applicable to problems with larger filter sizes.

As pointed out by [10, Fig. 4], the more efficient reductions in [5] do improve the speed of [8], but we observed at most a 1–2 second improvement when we used

them with [7]. The method presented in [10] also solves the individual pseudo-boolean problems better, but is slower. Two other approaches exist, but they are both significantly slower [11, 15].

While FoE denoising is a useful benchmark problem for discrete optimization, we should keep in mind that continuous methods can solve these problems much more efficiently.

REFERENCES

- [1] S. Agarwal and K. Mierle. *Ceres Solver: Tutorial & Reference*. Google Inc., 2012. <http://code.google.com/p/ceres-solver>.
- [2] Y. Boykov, O. Veksler, and R. Zabih. Fast approximate energy minimization via graph cuts. *Pattern Analysis and Machine Intelligence*, 23(11):1222–1239, 2001.
- [3] Y. Chen, T. A. Davis, W. W. Hager, and S. Rajamanickam. Algorithm 887: Cholmod, supernodal sparse cholesky factorization and update/downdate. *ACM Transactions on Mathematical Software (TOMS)*, 35(3):22, 2008.
- [4] D. Crandall, A. Owens, N. Snavely, and D. Huttenlocher. Discrete-continuous optimization for large-scale structure from motion. In *Conference on Computer Vision and Pattern Recognition*, 2011.
- [5] A. Fix, A. Gruber, E. Boros, and R. Zabih. A graph cut algorithm for higher-order markov random fields. In *International Conference on Computer Vision*, 2011.
- [6] H. Ishikawa. Higher-order clique reduction in binary graph cut. In *Conference on Computer Vision and Pattern Recognition*, 2009.
- [7] H. Ishikawa. Higher-order gradient descent by fusion-move graph cut. In *International Conference on Computer Vision*, 2009.
- [8] H. Ishikawa. Transformation of general binary MRF minimization to the first order case. *Pattern Analysis and Machine Intelligence*, 33(6):1234–1249, 2011.
- [9] J. Jancsary, S. Nowozin, and C. Rother. Loss-specific training of non-parametric image restoration models: A new state of the art. In *European Conference on Computer Vision*, 2012.
- [10] F. Kahl and P. Strandmark. Generalized roof duality. *Discrete Applied Mathematics*, 160(16–17):2419–2434, 2012.
- [11] X. Lan, S. Roth, D. Huttenlocher, and M. Black. Efficient belief propagation with learned higher-order markov random fields. *European Conference on Computer Vision*, 2006.
- [12] V. Lempitsky, C. Rother, S. Roth, and A. Blake. Fusion moves for markov random field optimization. *Pattern Analysis and Machine Intelligence*, 32(8):1392–1405, 2010.
- [13] D. Martin, C. Fowlkes, D. Tal, and J. Malik. A database of human segmented natural images and its application to evaluating segmentation algorithms and measuring ecological statistics. In *International Conference on Computer Vision*, 2001.
- [14] J. Nocedal and S. J. Wright. *Numerical Optimization*. Springer, 2006.
- [15] B. Potetz. Efficient belief propagation for vision using linear constraint nodes. In *Conference on Computer Vision and Pattern Recognition*, 2007.
- [16] S. Roth and M. J. Black. Fields of experts. *International Journal of Computer Vision*, 82(2):205–229, 2009.
- [17] B. Triggs, P. McLauchlan, R. Hartley, and A. Fitzgibbon. Bundle adjustment—a modern synthesis. *Vision algorithms: theory and practice*, pages 153–177, 2000.

(Petter Strandmark) GOOGLE INC., LUND UNIVERSITY
E-mail address: `petter@maths.lth.se`

(Sameer Agarwal) GOOGLE INC.
E-mail address, Corresponding author: `sameeragarwal@google.com`